Acta Cryst. (1984). A40, 297–305

Molecular Dynamics Simulation of Crystalline Naphthalene

BY R. G. DELLA VALLE* AND G. S. PAWLEY

Department of Physics, University of Edinburgh, Kings Buildings, Mayfield Road, Edinburgh EH9 3JZ, Scotland

(*Received* 8 *June* 1983; *accepted* 10 *January* 1984)

Abstract

A realistic molecular dynamics calculation for naphthalene is presented and a comparison is made between the simulation and the crystallographic data. The molecular dynamics sample consists of 4096 molecules arranged in a volume with cyclic boundary conditions, each molecule being associated with one processing element of the ICL DAP computer. The potential functions used are the same as those used for lattice dynamics, and are developed from atom–atom 6-exp functions. A comparison with a lattice dynamical result establishes the correctness of the program. Temperature is introduced in the usual molecular dynamics way, resulting in a true modelling of anharmonic behaviour. The calculation proceeds at zero pressure throughout, yielding the temperature variation of the crystalline unit cell, the mean molecular orientation and the rigid-body thermal vibration tensors **T** and **L**. These are compared with the recently reported results measured by neutron scattering from powder samples and analysed through constrained refinements. The variation of unit-cell volume with temperature is particularly close to the experimental result, though discrepancies begin to be significant in measurements involving the orientational behaviour of the molecules.

1. Introduction

In the early days of crystallography the main emphasis in structure determination was simply to solve the crystal structure, though even in those days there was considerable interest in the study of the thermal diffuse scattering. Nowadays some crystallographers are not satisfied unless they have studied the temperature variation of their structure, as this can yield new and useful information. Temperature is experimentally the most easily controlled state variable, though it is the most difficult variable to introduce into any model calculation. Only in recent years has it been possible to introduce temperature in any acceptable way as it is only recently that we have had enough computational resource to be able to perform extensive molecular dynamics calculations.

The work on the dynamics of crystalline naphthalene has so far been restricted to lattice dynamical work (Pawley, 1967, 1972; Mackenzie, Pawley & Dietrich, 1977; Schmelzer *et al.*, 1979, 1981; Natkaniec *et al.*, 1980; Dorner *et al.*, 1981), both calculations and measurements. The calculations are all based on the harmonic approximation, which makes the assumption that the molecular displacements are so small that anharmonic effects can be ignored. However, the potential function that is developed for these model calculations is a sum over a number of highly anharmonic functions, and so should be most appropriate for any calculation which treats the anharmonicity correctly. The measurements quoted above and the various structural studies (see Baharie & Pawley, 1982) contain some results made at various temperatures, giving excellent experimental results for comparison with model calculations. All this experimental work and the associated calculations have been done with fully deuterated naphthalene, and we continue to make this choice in these simulations.

For a system where anharmonicity is not enormous, it is possible to tackle the theoretical problem using Green-function (Maradudin & Fein, 1962) or Hamiltonian perturbation methods (Wallace, 1966). At low temperatures and for low frequencies the phonon anharmonicity is dominated by three- and four-phonon scattering processes. The scattering cross sections for such processes, and the resulting anharmonic frequency shifts and linewidths have been computed analytically for crystalline naphthalene in the temperature range below 68 K (Della Valle, Fracassi, Righini & Califano, 1983). The theory agrees reasonably well with the experimental data at low temperatures, but some discrepancies develop at higher temperatures. Such discrepancies would doubtless be reduced with the inclusion of fifth- and higher-order terms in the perturbation series. However, such additional terms are increasingly more complex and the fourth-order term appears to be the practical limit. Thus, such methods cannot give results in the regime of great interest near to a change of phase such as melting.

* Now returned to Istituto di Spettroscopia Molecolare, Università di Firenze, 50121 Firenze, Italy.

0108-7673/84/030297-09$01.50

The simplest form of model calculation in which temperature can properly be included and where a potential function is available is certainly molecular dynamics. For naphthalene such calculations have not been done until now, mainly due to the enormous amount of computation that is demanded by the size of the molecule. In the present work we make use of the highly parallel computer, the ICL DAP (distributed array processor), which is an array of 4096 processing elements, PEs, which function simultaneously. Each PE contains the information pertaining to one molecule, and so the smallest sample that the computer can use without degrading its efficiency is 4096. This is far greater than the number of molecules which are usually used in molecular dynamics studies, and as the molecule itself is much larger than most others used in a simulation of this kind, the present result represents a very considerable extension of the molecular dynamics field. The reader who wishes to know more about the DAP computer should consult the work of Gostick (1979) and the book by Hockney & Jesshope (1981), the details given later are simply those necessary for an understanding of the present simulation.

2. The molecular dynamics sample

Each of the PEs of the DAP contains information about one molecule, and the first calculation to be made in the simulation requires the distances between the atoms of one molecule and those of its neighbours to be found. Thus, each PE has to have access to the information in the PE which represents the neighbour, and with this information it can calculate all the intermolecular interatomic distances. These are required for the calculation of the forces between the various atoms. These forces are given by differentiating the total potential, assuming that the total potential is given by a sum over all atom–atom contacts of the form

$$V(r) = -Ar^{-6} + B\exp(-Cr). \qquad (1)$$

The constants used in this equation are those given by Williams (1967), Kitaigorodskii (1966) and Mackenzie, Pawley & Dietrich (1977), and are shown in Table 1. These will be referred to as W, K and M, respectively, in § 6 and in the figures.

The architecture of the DAP is such that the most convenient way of packing the molecules into the sample is by using a skew periodic boundary scheme. The PEs are arranged on a 64×64 lattice, with built-in cyclic boundary conditions, making any calculation in two dimensions very easy to implement. Each PE is directly connected to its four nearest neighbours, and can pass information to them or to any other PE *via* these four neighbours. To implement a three-dimensional sample it is possible to use the array as if it were a one-dimensional cyclic string, the skew conditions in three dimensions arising from the use of this string. The best way of explaining this is to describe the particular implementation that we have used for naphthalene.

Table 1. *Parameters for the intermolecular potential*

$$V(r) = -Ar^{-6} + B\exp(-Cr)$$

is the form of the atom–atom potential, with the following parameter values. Units are converted from those given in the references, and are J m^6/bond ($\times 10^{80}$) for *A*, J/bond ($\times 10^{20}$) for *B* and nm for *C*. The references are W (Williams, 1967), K (Kitaigorodskii, 1966), M (Mackenzie, Pawley & Dietrich, 1977).

	A			*B*			*C*		
	C–C	C–D	D–D	C–C	C–D	D–D	C–C	C–D	D–D
W	394	86	18	58122	6092	1844	0·360	0·367	0·374
K	248	107	39	29189	29189	29189	0·358	0·412	0·486
M	256	100	35	22055	22025	21997	0·333	0·393	0·478

The sample consists of 4096 molecules oriented in two possible symmetry-related ways and placed on centres of symmetry in the monoclinic space group $P2_1/a$. We choose to call the two orientations 'even' and 'odd', and there must be equal numbers of each orientation in the sample. The molecules are arranged on the cyclic string so that evens and odds alternate, and quite clearly this fits on to the string perfectly. There is one direction in the naphthalene structure where one can find a straight line which goes alternately through the centres of even and odd molecules such that one molecule is a nearest neighbour to the next. This is the [110] direction, and we choose this for the basis of the sample. In Fig. 1 the molecules 0, 1, 2 are arranged along this direction where the molecule labelled 0 could also be described as molecule 4096. Thus, in operation when PE number 1 finds the distances involving the molecule number 2, PE number 2 finds the equivalent information involving molecule number 3 simultaneously. The cyclic string property means that PE number 4096 simultaneously finds the information involving molecule number 1.

The three-dimensional nature of the packing is achieved as can be seen from the rest of Fig. 1. Even

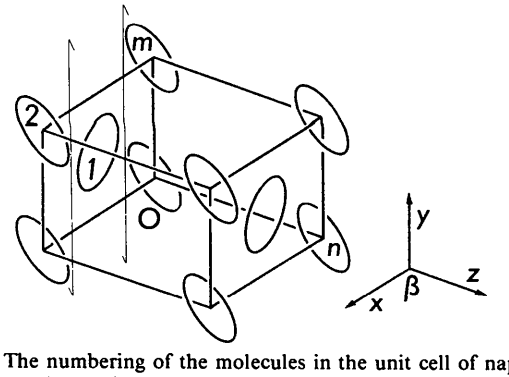

Fig. 1. The numbering of the molecules in the unit cell of naphthalene. The numbers *m* and *n* can be chosen to suit the problem, but must be even. The numbering establishes the relative position of the molecular information in the computer store.

numbers are chosen for m and n (*e.g.* $m=30$, $n=300$), and then the vector between molecule i and molecule $i+m$ is the crystal lattice vector **b**, and between i and $i+n$ is **c**. The lattice vector **a** is thus between molecule i and molecule $i-m+2$. All these molecule indices are modulo 4096, and i takes all values in the range 1–4096. The sample built up in this way fills space through the customary cyclic repetition, and although the unit sample is of a peculiar shape this does not have any disadvantages except perhaps in the analysis for phonon modes which has to be done in the reciprocal space (Pawley & Thomas, 1982).

3. Molecular dynamics

Thermal expansion is one of the more immediate consequences of anharmonicity. In cubic crystals the expansion tensor is isotropic and it is only necessary to adjust the lattice spacing to maintain a constant (usually zero) pressure. This is the procedure adopted by Pawley & Thomas (1982) in the simulation of SF_6, but is not adequate for the simulation of less-symmetric crystals. For a realistic simulation of a general system it is necessary to adjust all the lattice parameters to give zero stress in the sample, and one method for implementing this has been suggested by Parrinello & Rahman (1980). The method we have adopted allows the system to reach an equivalent equilibrium configuration; both methods involve approximations which become unimportant when the system equilibrates, and so there is no divergence between the two methods during the periods where observations are being made.

In our simulation the molecules are assumed to behave as rigid units under interactions with their near neighbours. The dynamical equations have been solved using Beeman's (1976) algorithm, while zero pressure has been maintained by changing the crystallographic unit cell so as to approach a free-energy minimum. Time stepping and strain relief have been alternated, readjusting the structure after a chosen number of dynamical time steps. This method therefore allows computational savings to be made when the system has reached an equilibrium, as the strain relief can then become an occasional step. Although the method of strain relief should not affect the equilibrated configuration, the details of the method are now outlined in brief.

In a system undergoing a homogeneous strain, the new positions of atoms are related to the old through the strain tensor u_{ij}:

$$r_i' = r_i + u_{ij} r_j. \tag{2}$$

If the strain is isotropic, $r'=(1+u)r$, and the volume V changes

$$V' = V + \mathrm{d}V = V + 3uV. \tag{3}$$

Such a strain involves a change in internal energy

$$\mathrm{d}U = T\,\mathrm{d}S - p\,\mathrm{d}V = T\,\mathrm{d}S - 3upV \tag{4}$$

in the isotropic case, or (Landau & Lifshitz, 1959)

$$\mathrm{d}U = T\,\mathrm{d}S - \sigma_{ij}\,\mathrm{d}u_{ij}, \tag{5}$$

where σ_{ij} is the stress tensor. In the isotropic case

$$\sigma_{ij} = pV\delta_{ij}. \tag{6}$$

In thermodynamic terms, with the free energy $F = U - TS$ we have

$$\sigma_{ij} = -\left(\frac{\partial U}{\partial u_{ij}}\right)_S = -\left(\frac{\partial F}{\partial u_{ij}}\right)_T. \tag{7}$$

The condition of constant (say zero) pressure is clearly that for a zero stress tensor. Ideally one would use the free-energy minimization to achieve this, but as the internal energy is more accessible we seek to minimize this quantity and accept that the entropy may change in the minimization search. This change should be small if the system is not near to a transition, and the effect of neglecting this change will be that the minimization search will be somewhat slower than otherwise.

The internal energy is a sum of a kinetic and a potential term

$$U = U_K + U_P = \tfrac{1}{2}\sum_{k=1}^{6N} M_k \dot{q}_k^2 + \tfrac{1}{2}\sum_{mn} \varphi[r(mn)], \tag{8}$$

M_k is a mass term associated with coordinate q_k, $r(mn)$ is the distance between atom m and atom n, and N is the total number of molecules, which have six degrees of freedom each. For the kinetic contribution we take an isotropic strain

$$\frac{\partial U_K}{\partial u_{ij}} = -pV\delta_{ij}, \tag{9}$$

obtaining the pressure *via* the virial theorem (Kittel, 1958),

$$pV = NkT - \frac{1}{3}\sum_{k=1}^{3}\left\langle \sum_{mn} \frac{\partial \varphi}{\partial r_k(mn)} r_k(mn)\right\rangle. \tag{10}$$

For the potential contribution,

$$\frac{\partial U_P}{\partial u_{ij}} = \frac{1}{2}\left\langle \sum_{mn} \frac{\partial \varphi}{\partial r_i(mn)} r_j(mn)\right\rangle, \tag{11}$$

as we have from the definition of u_{ij}

$$\partial r_k / \partial u_{ij} = \delta_{ik} r_j. \tag{12}$$

We thus have all the expressions needed for the strain tensor *via* the internal energy. This energy is minimized by a Newton–Raphson iterative steepest-descent method (see McGhee, 1967), giving the strain required to relieve the stress. At any one moment it is not necessary to iterate to completion as the approximations involved will cause the stress to vary

during subsequent steps, and it becomes most advantageous to interleave the Newton–Raphson iterations with the molecular dynamics time steps in such a way that the iterations have a diminishing role when the system equilibrates.

The interactions required for the molecular dynamics time step have been computed by summing over the 14 neighbour molecules inside a 9 Å range, approximating the remaining long-range part by an integral over a homogeneous medium. The free energy is differentiated numerically with respect to an arbitrary strain and the best strain in a parabolic approximation along the steepest direction is applied to the lattice. When the strain is completely relaxed the lattice symmetry fluctuates away from the monoclinic symmetry, and so a constraint is applied to keep the appropriate off-diagonal elements of the strain to zero. In the method just outlined it is easy to simulate any required crystallographic symmetry, though it is important that the fluctuations from the true symmetry that result from not having the constraint are such that the true symmetry is the time average. If it were not so this would be evidence for a structural phase transition which, in the present case, is not expected. The constraints applied to maintain the appropriate crystallographic symmetry could also be applied in the method of Parrinello & Rahman (1980).

Initially the system is set in motion using random velocities which correspond to the desired temperature. Correction for incorrect pressure is important at this stage, especially as the temperature needs constant readjustment as no randomly selected set of velocities (including angular velocities) can be expected to have the distribution of an equilibrated system. A number of time steps are therefore essential for equilibration at the chosen temperature. The time step chosen was 0·025 ps, a value small enough that energy non-conservation was not appreciable but large enough that the simulation became feasible. A clear statement of the time needed for equilibration to take place is not easy to give as each configuration was developed from an earlier configuration equilibrated either at a slightly different temperature or for a different potential function. However, in a particular case the change of temperature from 150 to 200 K showed a barely noticeable drift in the system parameters after 2·0 ps. This rather rapid equilibration is indicative of considerable anharmonicity, typical of a molecular crystal.

Estimation of the temperature is done by calculating the total kinetic energy and equating this to $3NkT$ ($N = 4096$). If the translational and rotational kinetic energies are used independently to estimate temperature, which has sometimes been done in gas- and liquid-phase simulations, the result from the rotational motion is very roughly $100/T\%$ larger (for T from 25 to 300 K) than that from the translational motion. This is consistent with the fact that a phonon description of the system becomes poorer with increasing temperature, as more anharmonicity is being introduced. At low temperatures the phonons are almost independent, and when this is true it is the mean phonon kinetic energy which should be equated to $\frac{1}{2}kT$, and as each phonon combines translational and rotational motion these simple motions cannot be considered independently. Such a simple division of the energy becomes progressively more valid as the temperature increases.

4. Quaternions

The angular motion of the molecules is treated using the quaternion formulation which has become accepted as the best method for molecular dynamics simulations (Evans, 1977). The great advantages of this formalism over the use of Eulerian angles are that the variable coordinates all behave in a similar fashion and that there is no possibility of singular behaviour. These advantages far outweigh the inconvenience of having four coordinates when there are only three degrees of freedom for a general rotation. The four coordinates have therefore to be constrained to be the coordinates of a unit vector in four dimensions or, in other words, to define a general point on the surface of a unit four-dimensional hypersphere. All four coordinates are varied according to the molecular dynamics algorithm for stepping in time and are then normalised to unity after each step. The basic equations for the use of quaternions are given by Du Val (1964), and some useful symmetry properties are presented by Pawley (1981). Only those properties that are necessary for the present paper will now be given.

The basic representation of a molecule is given in the principal-axis system. Let the quaternion that represents the rotation of such a standard molecule into the crystal orthogonal coordinate system to create an odd molecule of the sample be

$$q = (q_0; q_1, q_2, q_3). \tag{13}$$

Here we choose q_1, q_2, q_3 to be the coordinates for the imaginary prime (Du Val, 1964). A quaternion representing an even molecule is taken as $q' = (q'_0; q'_1, q'_2, q'_3)$, and this is converted to $(q_0; q_1, q_2, q_3)$ by rotation about the monoclinic diad axis as follows.

$$\begin{aligned}(q_0; q_1, q_2, q_3) &= (0; 0, 1, 0)(q'_0; q'_1, q'_2, q'_3)\\ &= (-q'_2; q'_3, q'_0, -q'_1).\end{aligned} \tag{14}$$

This can be checked using the rules in the cited references, but is easily seen to agree with the basic definition associating the quaternion with a rotation

matrix, thus:

$$(q_0; q_1, q_2, q_3) \equiv \begin{pmatrix} q_0^2+q_1^2-q_2^2-q_3^2 & 2(q_1q_2-q_3q_0) & 2(q_1q_3+q_2q_0) \\ 2(q_1q_2+q_3q_0) & q_0^2-q_1^2+q_2^2-q_3^2 & 2(q_2q_3-q_1q_0) \\ 2(q_1q_3-q_2q_0) & 2(q_2q_3+q_1q_0) & q_0^2-q_1^2-q_2^2+q_3^2 \end{pmatrix}. \quad (15)$$

After transforming the quaternions for the even molecules to coincide on average with the odd-molecule quaternions, the mean values can be calculated

$$Q_0=\langle q_0\rangle \quad Q_1=\langle q_1\rangle \quad Q_2=\langle q_2\rangle \quad Q_3=\langle q_3\rangle,$$

the averages being taken over all the 4096 molecules in the sample. These values are equivalent to a set of Eulerian angles (Φ, Θ, Ψ) through

$$\begin{aligned} Q_0&=\cos\Theta/2\cos(\Psi+\Phi)/2 \\ Q_1&=-\sin\Theta/2\cos(\Psi-\Phi)/2 \\ Q_2&=\sin\Theta/2\sin(\Psi-\Phi)/2 \\ Q_3&=-\cos\Theta/2\sin(\Psi+\Phi)/2. \end{aligned} \quad (16)$$

These Eulerian angles are as defined and used in the refinement of the powder diffraction data of Baharie & Pawley (1982), and the results of these experiments will be compared with the molecular dynamics results in Fig. 5.

5. The configurational averages

The molecular dynamics calculations give more than just the temperature variation of the mean molecular orientation. The second moments of the distribution of quaternions is closely related to the mean-square librational tensor, usually referred to as **L**. The first step towards getting **L** involves finding the quaternion p for each molecule which gives the difference between the corresponding q and the mean of q, namely Q. For this the inverse of Q is used as follows.

$$p=q(Q_0; -Q_1, -Q_2, -Q_3) \quad (17)$$

and as p is a small quaternion

$$p\doteq(1; \vartheta_1/2, \vartheta_2/2, \vartheta_3/2), \quad (18)$$

where ϑ_i are small angular rotations about the crystal orthogonal axes, which give directly

$$L_{ij}^{cr}=\langle\vartheta_i\vartheta_j\rangle. \quad (19)$$

Thus all the averages $\langle q_iq_j\rangle$ are found, from which all the tensor components of **L** can be found:

$$\begin{aligned} (\tfrac{1}{4})L_{11}^{cr}&=\langle q_0^2\rangle Q_1^2+\langle q_1^2\rangle Q_0^2+\langle q_2^2\rangle Q_3^2+\langle q_3^2\rangle Q_2^2 \\ &\quad -2\{\langle q_0q_1\rangle Q_0Q_1-\langle q_0q_2\rangle Q_1Q_3+\langle q_0q_3\rangle Q_1Q_2 \\ &\quad +\langle q_1q_2\rangle Q_0Q_3-\langle q_1q_3\rangle Q_0Q_2+\langle q_2q_3\rangle Q_2Q_3\} \\ (\tfrac{1}{4})L_{23}^{cr}&=[\langle q_0^2\rangle-\langle q_1^2\rangle]Q_2Q_3+[\langle q_2^2\rangle-\langle q_3^2\rangle]Q_0Q_1 \\ &\quad +\langle q_0q_1\rangle(Q_2^2-Q_3^2)+\langle q_2q_3\rangle(Q_0^2-Q_1^2) \\ &\quad +[\langle q_1q_2\rangle+\langle q_0q_3\rangle](Q_1Q_3-Q_0Q_2) \\ &\quad +[\langle q_1q_3\rangle-\langle q_0q_2\rangle](Q_1Q_2+Q_0Q_3). \end{aligned} \quad (20)$$

The advantage of these equations is that all the quaternion moments $\langle q_iq_j\rangle$ can be found during the simulation runs independently of the evaluation of the mean quaternion Q, and the calculation can be run in stages until sufficient statistics have been collected. The results obtained in these simulations have been taken at 64 steps from fully equilibrated runs. This is clearly not a sampling of independent configurations, but such a condition is not necessary for the quantities we are here measuring. The results are presented and discussed in the next section, where the librational tensor in molecular coordinates, $\mathbf{L}^{mol}$, is also considered. This tensor is given by a different combination of quaternion moments:

$$\begin{aligned} (\tfrac{1}{4})L_{11}^{mol}&=\langle q_0^2\rangle Q_1^2+\langle q_1^2\rangle Q_0^2+\langle q_2^2\rangle Q_3^2+\langle q_3^2\rangle Q_2^2 \\ &\quad -2\{\langle q_0q_1\rangle Q_0Q_1+\langle q_0q_2\rangle Q_1Q_3-\langle q_0q_3\rangle Q_1Q_2 \\ &\quad -\langle q_1q_2\rangle Q_0Q_3+\langle q_1q_3\rangle Q_0Q_2+\langle q_2q_3\rangle Q_2Q_3\} \\ (\tfrac{1}{4})L_{23}^{mol}&=[\langle q_0^2\rangle-\langle q_1^2\rangle]Q_2Q_3-[\langle q_2^2\rangle-\langle q_3^2\rangle]Q_0Q_1 \\ &\quad -\langle q_0q_1\rangle(Q_2^2-Q_3^2)+\langle q_2q_3\rangle(Q_0^2-Q_1^2) \\ &\quad +[\langle q_1q_2\rangle-\langle q_0q_3\rangle](Q_1Q_3+Q_0Q_2) \\ &\quad +[\langle q_1q_3\rangle+\langle q_0q_2\rangle](Q_1Q_2-Q_0Q_3). \end{aligned} \quad (21)$$

Presenting this equation emphasises the fact that the important measures to be made are of the fundamental correlation functions, from which various quantities can be constructed when the simulation is completed.

6. Simulation results

A program was written to perform the simulation described above, and it was thought to be wise to devise a test for it. This was furnished by an independent lattice-dynamical calculation with the same potential function, giving eigenvectors for modes of any chosen wavelength. One mode at 1·54 THz at the Γ point (infinite wavelength) corresponded to almost pure libration about the major inertia axis and so we set up the molecular dynamics sample with molecules displaced about their major axes all by equal amounts. The simulation then produced the variation of this displacement as a function of time as shown in Fig. 2. Although this figure shows contamination from other Γ modes, the dominant mode shows an oscillation of the correct frequency, substantiating the accuracy of the program. A full analysis of the phonon spectrum, however, is beyond the scope of the present paper as it requires a far greater amount of computation, but it is nevertheless now entirely feasible.

The clearest indication of the existence of anharmonicity in crystal systems is given by thermal expansion. Our first task is therefore to investigate the variation of unit-cell volume and shape with temperature. We have no reason to expect *a priori* that the simulation will yield a result which mirrors reality in any way for the anharmonic phenomena, although the potential functions used have been fitted to a wide variety of data on the assumption that a universal interaction function actually exists. The results will be presented in terms of diagrams, in which results for the three different potential functions will be presented.

The variation of the unit-cell volume with temperature is shown in Fig. 3. This includes the experimental result *E*, taken from the powder neutron diffraction study of naphthalene-d_8 by Baharie & Pawley (1982). The experimental curve has been extrapolated to 353·3 K, the melting temperature of the material (Sherwood, 1983). The curves for W and K follow experiment very faithfully, at approximately 1·5% excess volume. The experimental non-linearity at very low temperatures is caused by the zero-point motion which is not negligible below the Debye temperature of roughly 100 K; there is no way in which this effect can be included in a classical computer simulation and therefore the calculation shows a more rapid expansion than experiment at low temperatures.

Within the temperature range of the solid it is clear that potential M produces too rapidly an increasing volume. This is expected to be caused by the fact that the potential was found by a fitting to the phonon measurements made at liquid-nitrogen temperatures, not near absolute zero. The configurations for M, being the first set fully equilibrated, were used as starting configurations for W and then W were used to initiate K at a given temperature. Above 325 K this led to a peculiar artefact of the simulation which might be related in some way to melting as the amplitude of motion in this temperature region became so large that some important new intermolecular interactions were being omitted. This is indicative of a problem we face on DAP architecture computers – if a rare interaction is sometimes needed in the calculation then this interaction has to be included for the whole of the system ideally for all of the time, and the consequent computational demand increases disproportionately.

These arguments suggest that M predicts melting at <300 K, W and K somewhere about 325 K, suggesting that W or K are very appropriate potential functions for naphthalene simulations. We need to look at other phenomena in order to decide which is the better, although lattice dynamical studies favour W.

Fig. 4 shows the variation of the unit-cell constants with temperature for the W potential function. This should be compared with the experimental result of Baharie & Pawley (1982). The closest agreement between the unit-cell lengths and experiment is given by the M potential (results not presented), but the monoclinic angle does not agree well, giving a poor comparison with the total cell volume. For W (and to some extent K) the monoclinic angle counteracts the cell-length discrepancies, but shows considerably more temperature variation than exists in the natural state. Thus, W gives rise to a very acceptable molecular volume but does not fully describe the orientational forces.

The orientation of the molecule in the crystal can be described either in terms of quaternions or Euler

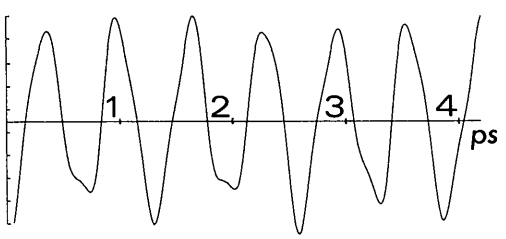

Fig. 2. Variation of angular displacement of one (and therefore every) molecule about its major inertia axis as a function of time in a system set up to oscillate in almost a pure mode, showing predominantly the librational mode about this axis of frequency 1·54 THz.

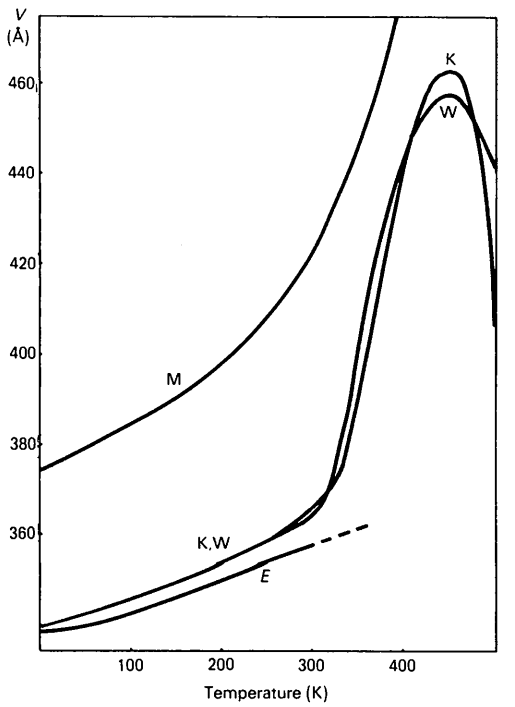

Fig. 3. Variation of the total unit-cell volume with temperature. *E*: experiment (after Baharie & Pawley, 1982) extrapolated to the melting point of 353·3 K (Sherwood, 1983). W, K and M refer to the potential functions as given in Table 1. The values have been calculated at 1, 25, 50, 100, 150, 200, 250, 300 K, and then in steps of 25 to 500 K. The standard deviations associated with each point do not exceed the width of the line on the diagram.

angles, as we have seen above. The experimental results have been obtained with the latter description and, as this involves the fewer parameters, we use this description for the analysis of the variation of molecular orientation with temperature. This is shown in Fig. 5, which includes the experimental results tabulated by Baharie & Pawley (1982). W is better than K for only one Euler angle, but none of the potentials give rise to a good agreement with the experimental temperature variation. Again we see that the variation predicted by all the potentials is greater than observed, from which we must conclude that there is an important part of the potential function missing from those used, which would tend to stabilise the molecular orientation. Such a potential is most probably the quadrupole–quadrupole interaction associated with the π-electron system known to be of importance in naphthalene (Della Valle *et al.*, 1983). Inclusion of a quadrupole interaction in the present work would extend the calculation beyond our present computational capacity.

From the simulation we can readily calculate the crystallographic mean-square translational (**T**) and librational (**L**) tensors. The diagonal values for **L** when expressed in the crystal orthogonal coordinate system are plotted in Fig. 6 for the three different potentials. These are given separately and to scale with the plots of the experimental results of Baharie & Pawley (1982) which are in the same coordinate system; this system corresponds quite closely to the principal-axis coordinate system. All the potentials agree with the experimental result that the largest libration amplitude takes place about the axis of greatest inertia. Detailed comparison with experiment is not easy to present, but a good picture can be got

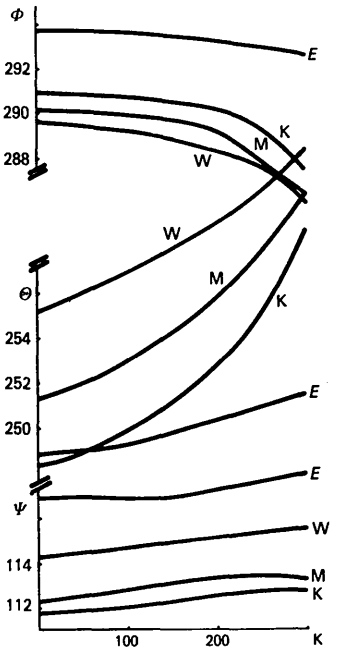

Fig. 5. The variation of the Euler angles which describe the molecular orientation as a function of temperature. The lettering corresponds to Fig. 3. The temperatures for the results are as for Fig. 4, and again the standard deviations are too small to be represented.

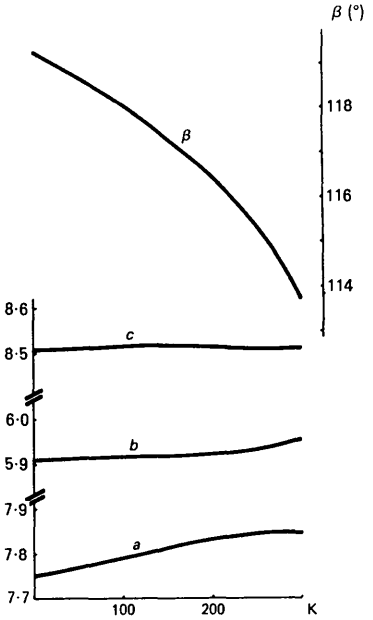

Fig. 4. Variation of the unit-cell constants with temperature for W. This figure corresponds to that presented by Baharie & Pawley (1982). The temperatures for the results are as for Fig. 3 up to 300 K, and again the standard deviations are too small to be represented.

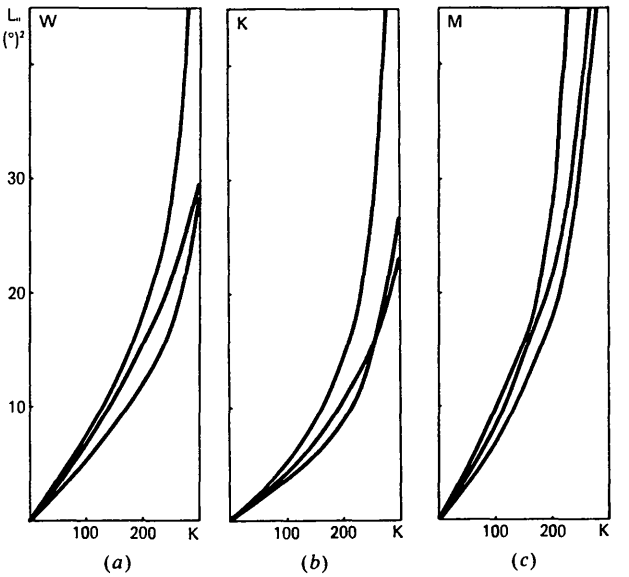

Fig. 6. The variation of the mean-square librational tensor principal values with temperature, (*a*) W, (*b*) K and (*c*) M. L_{11} is the greatest everywhere, and L_{22} is the least except for K above 250 K. The temperatures for the results are as for Fig. 4, and again the standard deviations are too small to be represented.

from Fig. 7 which contains the variation of the traces of **T** and **L** with temperature for the three potentials and for experiment. From Fig. 7 we see that all the simulations predict a more rapid increase of amplitude with temperature for both **T** and **L** than is observed from the neutron powder diffraction studies, though it must be borne in mind that this discrepancy is at temperatures over twice the Debye temperature for this sytem which is approximately 100 K.

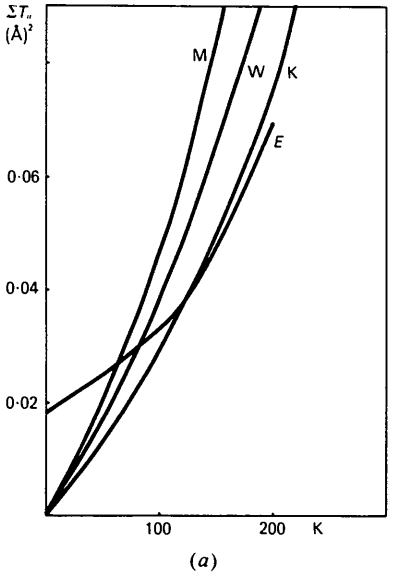

(*a*)

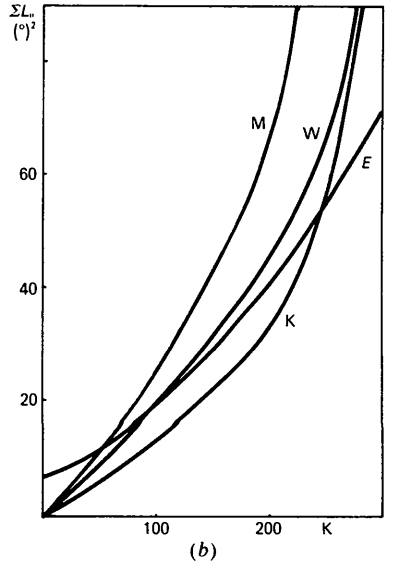

(*b*)

Fig. 7. The variation of the trace of (*a*) **T** and (*b*) **L** as a function of temperature for the three potential functions and for experiment. The lettering corresponds to Fig. 3. Again L_{11} is the greatest and L_{22} the least; T_{33} is the greatest and T_{22} the least as in the experimental result. The temperatures for the results are as for Fig. 4, and again the standard deviations are too small to be represented.

7. Conclusion

The best test which can now be made of the potential used in this simulation surely involves the study of the melting phenomenon. Although the potential functions have been shown to be inadequate as far as the fine detail of the molecular orientational behaviour is concerned, such considerations are likely to be less important when the thermal disordering approaches that required for melting. At this point the neglect of the quadrupole–quadrupole interactions would be more justifiable and a realistic simulation could be made even with these simple potentials. However, such a simulation would require much more computational resource than has been used here as the number of molecular interactions to be calculated would be considerably larger. The present calculation itself involves the determination of approximately 10^7 interactions at each time step. Nevertheless, it is possible that the peculiar behaviour of Fig. 3 is pointing towards the melting transition, and this is currently being investigated.

We wish to thank the Science and Engineering Research Council (UK) for financial support in purchasing the DAP at Edinburgh which was used for these calculations, and the European Research Office of the US Army for the full support of one of us (RGD).

References

BAHARIE, E. & PAWLEY, G. S. (1982). *Acta Cryst.* A**38**, 803–810.
BEEMAN, D. (1976). *J. Comput. Phys.* **20**, 130–139.
DELLA VALLE, R. G., FRACASSI, P. F., RIGHINI, R. & CALIFANO, S. (1983). *Chem. Phys.* **74**, 179–195.
DORNER, B., BOKHENKOV, E. L., SHEKA, E. F., CHAPLOT, S. L., PAWLEY, G. S., KALUS, J., SCHMELZER, U. & NATKANIEC, I. (1981). *J. Phys. (Paris)* **42**, C6, 602–604.
DU VAL, P. (1964). *Homographies, Quaternions and Rotations.* Oxford Mathematical Monograph.
EVANS, D. J. (1977). *Mol. Phys.* **34**, 317–323.
GOSTICK, H. (1979). *ICL Tech. J.* **1**, 116–135.
HOCKNEY, R. W. & JESSHOPE, C. R. (1981). *Parallel Computers.* Bristol: Adam Hilger Ltd.
KITAIGORODSKII, A. I. (1966). *J. Chim. Phys.* **63**, 9–16.
KITTEL, C. (1958). *Elementary Statistical Physics.* New York: Wiley.
LANDAU, L. D. & LIFSHITZ, E. M. (1959). *Theory of Elasticity.* London: Pergamon Press.
MCGHEE, R. B. (1967). In *Digital Computer Users' Handbook*, edited by M. KLEVER & G. A. KORN, ch. 4.8. New York: McGraw-Hill.
MACKENZIE, G. A., PAWLEY, G. S. & DIETRICH, O. W. (1977). *J. Phys. C*, **10**, 3723–3736.
MARADUDIN, A. A. & FEIN, A. E. (1962). *Phys. Rev.* **128**, 2589–2608.
NATKANIEC, I., BOKHENKOV, E. L., DORNER, B., KALUS, J., MACKENZIE, G. A., PAWLEY, G. S., SCHMELZER, U., & SHEKA, E. F. (1980). *J. Phys. C*, **13**, 4265–4283.
PARRINELLO, M. & RAHMAN, A. (1980). *Phys. Rev. Lett.* **45**, 1196–1199.
PAWLEY, G. S. (1967). *Phys. Status Solidi* **20**, 347–360.

PAWLEY, G. S. (1972). *Phys. Status Solidi* **B49**, 475–488.
PAWLEY, G. S. (1981). *Mol. Phys.* **43**, 1321–1330.
PAWLEY, G. S. & DOVE, M. T. (1983). *Proceedings of the 3rd General Conference of the Condensed Matter Division of the EPS*, edited by W. CZAJA & A. THOMAS, pp. 583–592. Basel: Birkhäuser.
PAWLEY, G. S. & THOMAS, G. W. (1982). *J. Comput. Phys.* **47**, 165–178.
SCHMELZER, U., BOKHENKOV, E. L., DORNER, B., KALUS, J., MACKENZIE, G. A., NATKANIEC, I., PAWLEY, G. S. & SHEKA, E. F. (1981). *J. Phys. C*, **14**, 1025–1041.
SCHMELZER, U., DORNER, B., KALUS, J., NATKANIEC, I., OSTERTAG, R., PAWLEY, G. S., MACKENZIE, G. A., SHEKA, E. F. & BOKHENKOV, E. L. (1979). *Phys. Status Solidi*, **B91**, K27–29.
SHERWOOD, J. N. (1983). Private communication.
WALLACE, D. C. (1966). *Phys. Rev.* **152**, 247–260.
WILLIAMS, D. E. (1967). *J. Chem. Phys.* **47**, 4680–4684.

SHORT COMMUNICATIONS

Contributions intended for publication under this heading should be expressly so marked; they should not exceed about 1000 *words; they should be forwarded in the usual way to the appropriate Co-editor; they will be published as speedily as possible.*

Acta Cryst. (1984). **A40**, 305–306

Determination of the positions of anomalous scatterers: probabilistic coefficients for a Patterson synthesis.

By G. CASCARANO and C. GIACOVAZZO, *Istituto di Mineralogia e Petrografia, Universitá Palazzo Ateneo,* 70121 *Bari, Italy*

(*Received* 14 *June* 1983; *accepted* 4 *November* 1983)

Abstract

The conditional joint probability distribution of the phase $\varphi = \varphi_{\mathbf{h}} + \varphi_{-\mathbf{h}}$ given $|F^+|$, $|F^-|$ is used in order to suggest coefficients for a Patterson synthesis for the determination of the positions of anomalous scatterers. A theoretical comparison with Rossmann's approach [Rossmann, M. G. (1981). *Acta Cryst.* **14**, 383–388] is made.

Definitions

N	number of atoms in the unit cell
$f = f' + if''$	general expression for the atomic scattering factor; f' and f'' are its real and imaginary parts
F^+, F^-	structure factors of the reflexions **h** and $-\mathbf{h}$, respectively
R^+, φ^+, R^-, φ^-	normalized structure factor and phase of the reflextion **h** and $-\mathbf{h}$, respectively
$\Sigma = \sum_{j=1}^{N} (f_j'^2 + f_j''^2)$	average value of $\lvert F_{\mathbf{h}}\rvert^2$ at a given $\lvert\mathbf{h}\rvert$
$c_1 = \sum_{j=1}^{N} (f_j'^2 - f_j''^2)/\Sigma$	
$c_2 = 2\sum_{j=1}^{N} f_j' f_j''/\Sigma$	
$c = [1 - (c_1^2 + c_2^2)]^2$	
$\Phi = \varphi^+ + \varphi^-$	
$F'' = \sum_{j=1}^{N} f_j'' \exp(2\pi i \mathbf{hr}_j)$	
F^0	structure factor (imaginary component of anomalous dispersion omitted)

An important application of the observed anomalous scattering for the determination of the positions of the anomalous scatterers has been described by Rossmann (1961). In his approach a Patterson synthesis with $(|F^+| - |F^-|)^2$ coefficients is used which will produce peaks at the ends of vectors that relate anomalous scatterers. The 'best' *ad hoc* Patterson synthesis (having $|F''|^2$ coefficients) is not available from one-wavelength techniques: thus Rossmann's coefficients can be considered a useful approximation of the 'best' coefficients. The approximation is good if the Petsko (1976) approximation holds (see Fig. 1):

$$|F^0| \simeq \tfrac{1}{2}(|F^+| + |F^-|). \quad (1)$$

Indeed, if we replace (1) in

$$|F^0|^2 = \tfrac{1}{2}[|F^+|^2 + |F^-|^2] - |F''|^2, \quad (2)$$

(3) is obtained:

$$|F''|^2 \simeq \tfrac{1}{4}(|F^+| - |F^-|)^2. \quad (3)$$

Relation (1) holds if Φ is small enough, that is to say, if $|F''|$ is small compared with $|F^+|$ and $|F^-|$. Such conditions are not always fulfilled, especially if: (*a*) synchrotron radiation is used; indeed the anomalous components of the

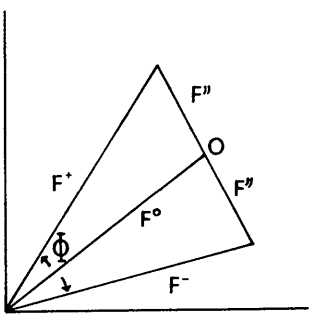

Fig. 1. Argand diagram in the case of anomalous scattering.

0108-7673/84/030305-02$01.50